

Measurement of Dielectric and Magnetic Properties of Ferromagnetic Materials at Microwave Frequencies

By WILHELM VON AULOCK and JOHN H. ROWEN

(Manuscript received August 15, 1956)

Some experimental techniques are discussed which permit measurement of the magnetic and dielectric properties of ferrite materials in the microwave region by observing the perturbation in a cylindrical cavity due to insertion of a small ferrite sample. A comparison of the properties of thin disc samples with those of small spheres shows that discs yield more accurate results in the region below ferromagnetic resonance whereas spheres are preferable for the study of ferrite properties near resonance. A short description of instrumentation for cavity measurements at 9,200 mc is given and experimental results of disc measurements are reported for a low-loss BTL ferrite and several disc diameters. A comparison of experimental results with Polder's theory indicates that the loss of polycrystalline ferrites below resonance is considerably lower than that predicted from an evaluation of the width of the resonance absorption line.

1. INTRODUCTION

The dielectric and magnetic properties of semi-conducting ferromagnetic materials such as ferrites have been the subject of intense study in recent years. Analytical expressions for the components μ and κ of the permeability tensor of a loss-free single-crystal ferrite were derived by Polder.¹ These expressions were later modified to include a loss factor α .^{2, 3} Yager and others⁴ measured the resonance absorption of single crystals of nickel ferrite and found very good agreement with theory provided the loss factor α was determined from the width of the measured resonance absorption line. However, when Artman and Tannenwald⁵ measured the real and imaginary parts of μ and κ for polycrystalline ferrites they found that agreement with theory was somewhat less than perfect if α was also determined from the measured line width. Discrepancies were observed for both real and imaginary parts of $\mu +$

κ in the region below resonance because the effects of polycrystalline structure and anisotropy forces were neglected in Polder's and Hogan's² analysis. Furthermore, it was assumed in the derivation of the permeability tensor that the ferrite is saturated with a biasing dc magnetic field which is large compared to the microwave magnetic field.

There exists a great need for experimental data for all those conditions where some of the above assumptions do not hold. In particular, the region of biasing magnetization between zero and ferromagnetic resonance is of interest because it is the operating region for many ferrite devices such as phase shifters, modulators, and field displacement isolators. Techniques for the measurement of ferrite parameters below resonance were investigated and it was found that the measurement of the perturbation of a degenerate cylindrical cavity by a thin ferrite disc yielded accurate results, whereas observation of the cavity perturbation caused by a small sphere produced less accurate data.

It is the purpose of this paper to describe and discuss the thin disc method and to compare it with other techniques described in the literature.^{5, 7} After defining the ferrite parameters as constants in Maxwell's equations it is shown how these parameters can be obtained from various measuring techniques. Instrumentation for the thin disc technique is described and a few remarks are made pertaining to experimental difficulties. Finally, some measurements of low-loss ferrites are reported and compared with values predicted by Polder's relations.

2. DESCRIPTION OF FERRITE PARAMETERS

It is customary⁸ to define the electric and magnetic polarization vectors \vec{P} and \vec{M} in terms of the field vectors \vec{E} (electric field intensity), \vec{D} (electric displacement), \vec{H} (magnetic field intensity), and \vec{B} (magnetic induction). In the M.K.S. system we have:

$$\vec{P} = \vec{D} - \epsilon_0 \vec{E}$$

$$\vec{M} = \vec{B}/\mu_0 - \vec{H}$$

$\epsilon_0 = 8.854 \times 10^{-12}$ farad/meter, permittivity of free space

$\mu_0 = 4\pi \times 10^{-7}$ henry/meter, permeability of free space

Then, the intrinsic parameters of a ferrite medium are defined as those quantities which relate \vec{P} and \vec{M} to the electric and magnetic fields in the medium respectively.

$$\vec{P} = \epsilon_0 \chi_e \vec{E}$$

$$\vec{M} = \vec{\chi}_m \vec{H}$$

Whereas the electric susceptibility χ_e is a scalar quantity in ferrites the

magnetic susceptibility $\overleftrightarrow{\chi}_m$ is known to have tensor properties. Assuming that the static magnetic field H_z is in the z -direction we have

$$\overleftrightarrow{\chi}_m = \begin{vmatrix} \chi_m & -j\kappa & 0 \\ j\kappa & \chi_m & 0 \\ 0 & 0 & 0 \end{vmatrix} \quad (1)$$

If we restrict ourselves to sinusoidal time variation of the RF fields we may describe electric and magnetic losses in the ferrite by regarding χ_e , χ_m , and κ as complex quantities:

$$\begin{aligned} \chi_e &= \chi_e' - j\chi_e'' \\ \chi_m &= \chi_m' - j\chi_m'' \\ \kappa &= \kappa' - j\kappa'' \end{aligned}$$

Thus, it is seen that the RF properties of a ferrite medium regardless of geometry are completely described by six "intrinsic" parameters, χ_e' , χ_e'' , χ_m' , χ_m'' , κ' , and κ'' . The dielectric constant ϵ and permeability $\overleftrightarrow{\mu}$ of the material are obtained from

$$\begin{aligned} \epsilon &= \chi_e + 1 \\ \overleftrightarrow{\mu} &= \overleftrightarrow{\chi}_m + 1 \end{aligned}$$

where $\mathbf{1}$ is the unit matrix.

It is the objective of the measurement to obtain each of the above parameters as a function of one or more variables of interest such as frequency, saturation magnetization, static magnetic field, temperature, applied power and others. Measurements may be made on single ferrite crystals — mostly for research purposes — or on polycrystalline material for many purposes in connection with the development of ferrite materials and devices. These measurements are generally compared to the behavior of χ_m and κ as predicted by Polder's equations. One obtains from the equation of motion of magnetization¹

$$\begin{aligned} \chi_m &= \mu - 1 = \frac{\gamma^2 M_z H_z}{\gamma^2 H_z^2 - \omega^2} \\ \kappa &= -\frac{\omega |\gamma| M_z}{\gamma^2 H_z^2 - \omega^2} \end{aligned}$$

Using Suhl and Walker's³ notation this may be written as

$$\begin{aligned} \chi_m &= \frac{p\sigma}{\sigma^2 - 1} \\ \kappa &= -\frac{p}{\sigma^2 - 1} \end{aligned}$$

where $p = |\gamma| M_z/\omega$ normalized saturation magnetization

$\sigma = |\gamma| H_z/\omega$ normalized static magnetic field in the ferrite

$|\gamma| = 2.8$ me per oersted, gyromagnetic ratio

$\omega =$ operating frequency

It appears that some cavity techniques measure the eigenvalues of (1), $\chi_m + \kappa$ and $\chi_m - \kappa$, directly, which are seen to be

$$\chi_m \pm \kappa = \frac{p}{\sigma \pm 1} \quad (2)$$

Suhl and Walker show that a loss term may be introduced by replacing σ by $\sigma + j\alpha(\text{sgn } p)$ in (2).^{*} Separating real and imaginary parts we get

$$\chi_m' \pm \kappa' = \frac{p(\sigma \pm 1)}{(\sigma \pm 1)^2 + \alpha^2} \quad (3)$$

$$\chi_m'' \pm \kappa'' = \frac{\alpha p(\text{sgn } p)}{(\sigma \pm 1)^2 + \alpha^2} \quad (4)$$

For the determination of α from measurements it is convenient to define a loss tangent

$$\delta_{\pm} \equiv \frac{\chi_m'' \pm \kappa''}{\chi_m' \pm \kappa'} = \frac{\alpha(\text{sgn } p)}{\sigma \pm 1} \quad (5)$$

Typical curves for $\chi_m \pm \kappa$ and δ_{\pm} assuming $p = 0.5$ and $\alpha = 5 \times 10^{-2}$ are shown on Figure 1.[†] For the purpose of describing and comparing experimental results, it may be convenient to distinguish among various regions of H_z as indicated on the graph because a different measurement technique may be required for accurate measurements in each region.

3. METHODS FOR MEASURING MAGNETIC PROPERTIES

Three measurement methods have been reported in the literature all of which employ the detuning and change in $1/Q$ of a resonant cavity by a small ferrite sample. Van Trier⁷ used very thin long cylindrical samples in a coaxial cavity. Artman and Tannenwald⁵ employed small spheres, and we used thin discs⁹ both placed close to the endwall of a cylindrical degenerate cavity excited by a TE_{111} mode (Figs. 2 and 3). Recently, Berk and Lengyel⁶ suggested the use of a cylindrical post at the center

^{*} By definition $\text{sgn } p = +1$ for $p > 0$ and $\text{sgn } p = -1$ for $p < 0$.

[†] Since it is customary to use $\chi_m + \kappa$ for the designation of the resonance line this notation has been used here. Consequently, p and σ should be assumed negative.

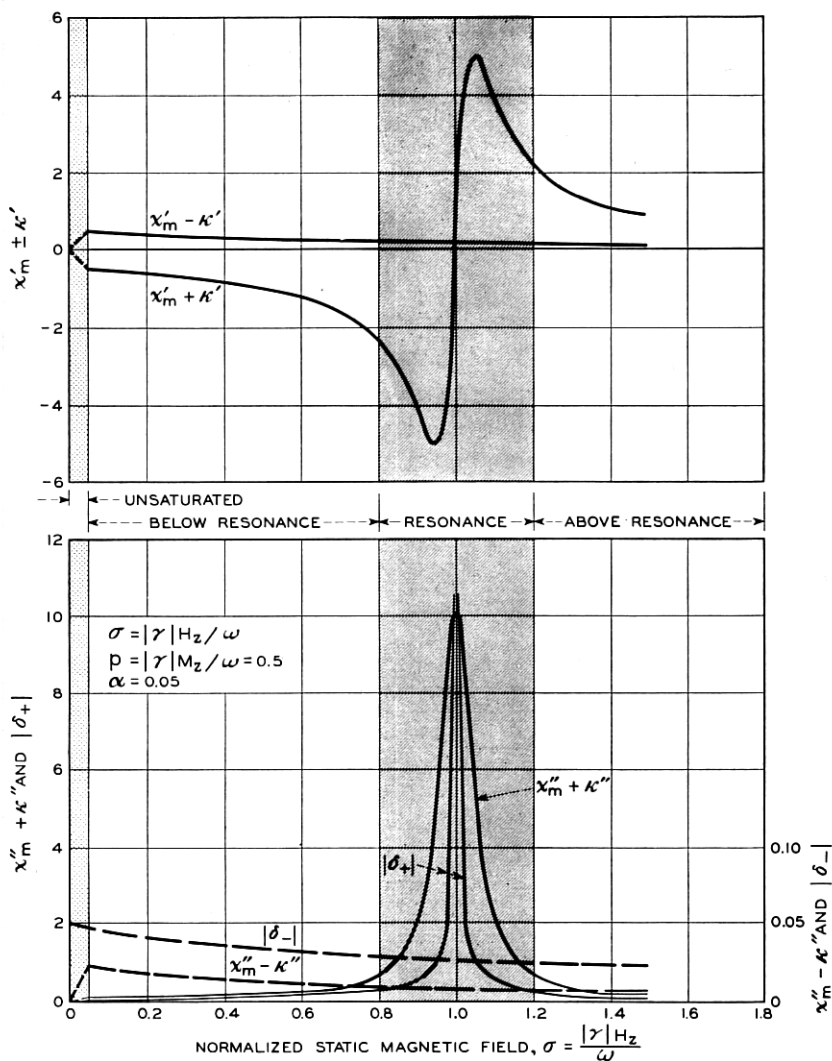


Fig. 1 — Theoretical values of $\chi_m \pm \kappa$ and loss tangent δ_{\pm} versus normalized static field σ .

of a degenerate rectangular cavity.* In principle, all these methods permit the determination of the six parameters $\chi'_e, \chi''_e, \chi'_m, \chi''_m, \kappa',$ and κ'' . However, in practical applications there are significant differences, e.g.,

* As this paper was being written another variation of the thin cylinder technique using the TM_{110} mode in a circular cavity was reported by Spencer and LeCraw at the I.R.E. Convention, New York, Mar. 21, 1956.

between the use of a spherical sample and a thin disc, such as the perturbing effect on the cavity field, the accuracy of small loss measurement, the occurrence of resonance at a static field where the intrinsic parameters are not at resonance,¹⁰ and the possibility of making accurate measurements of the electric susceptibility. Therefore, the sphere method and the disc method will be reviewed briefly and an attempt will be made to compare their capabilities. It is hoped that this comparison will also be helpful for the evaluation of other measuring techniques not covered in this paper.

3.1 The Small Sphere Method

In order to appreciate the significance of the quantities measured with the small sphere method it is expedient to define an effective susceptibility tensor $\vec{\chi}_{ms}$ by relating the magnetization vector* to the applied

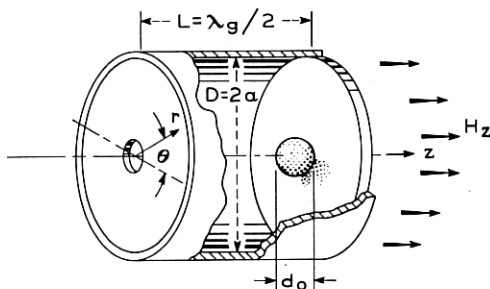


Fig. 2 — Degenerate TE_{111} cylindrical cavity with ferrite sphere.

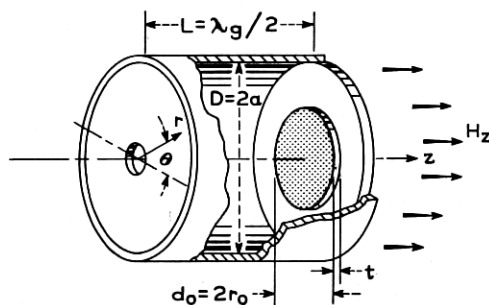


Fig. 3 — Degenerate TE_{111} cylindrical cavity with ferrite disc.

* R. A. Waldron (Institute of Electrical Engineers, Convention Oct. 29 to Nov. 2, on Ferrites, London, 1956) related the magnetic induction vector \vec{B} in a

field \vec{H}^0

$$\vec{M} = \vec{\chi}_{ms} \vec{H}^0$$

and observing that the RF components of \vec{M} and \vec{H}^0 (denoted by lower case letters) are related in a cylindrical coordinate system by

$$\begin{aligned} m_r &= \chi_{ms} h_r^0 - j\kappa_s h_\theta^0 \\ m_\theta &= j\kappa_s h_r^0 + \chi_{ms} h_\theta^0 \end{aligned} \quad (6)$$

Placing the small ferrite sphere close to the endwall of the cavity (Fig. 2) and observing the splitting of the resonance into two frequencies ω_\pm (related to the positive and negative circularly polarized modes) and the two changes in $1/Q$ of the cavity after application of a static magnetic field in the axial direction leads to two measurable quantities

$$\Delta\omega_\pm = \omega_0 - \omega_\pm \quad \text{frequency shift}$$

$$\Delta(1/Q)_\pm = 1/Q_\pm - 1/Q_0 \quad \text{change in internal } Q \text{ of the cavity}$$

where ω_0 and Q_0 are resonance frequency and Q of the empty cavity. It can be shown that real and imaginary part of χ_{ms} and κ_s can be obtained from†

$$\frac{2\Delta\omega_\pm}{\omega_0} = 0.6982 \frac{\lambda_0^2}{D^2} \cdot \frac{d_0^3}{L^3} (\chi_{ms}' \pm \kappa_s') \quad (7)$$

$$\Delta(1/Q)_\pm = 0.6982 \frac{\lambda_0^2}{D^2} \cdot \frac{d_0^3}{L^3} (\chi_{ms}'' \pm \kappa_s'') \quad (8)$$

The quantities d_0 , D , and L are the sphere diameter, cavity diameter and length respectively, λ_0 is the wavelength in free space associated with ω_0 . In order to obtain the intrinsic parameters χ_m and κ from (7) and (8) one may use the relationships⁶

$$\vec{H}^0 = \vec{H} + \vec{M}/3 \quad (9)$$

$$\chi_{ms} \pm \kappa_s = \frac{3(\chi_m \pm \kappa)}{\chi_m \pm \kappa + 3} \quad (10)$$

sphere to the applied field by writing $\frac{1}{\mu_0} \vec{B} = \vec{\mu}_s \vec{H}^0$ where $\vec{\mu}_s$ may be designated the external relative permeability tensor. It can be readily shown that Waldron's results are in agreement with ours if one notes that $(2/3)\vec{\chi}_{ms} = \vec{\mu}_s - \mathbf{1}$. We found that the use of the effective susceptibility tensor $\vec{\chi}_{ms}$ is much to be preferred over $\vec{\mu}_s$ because it simplifies notation and interpretation of experimental results in terms of the intrinsic quantities χ_m and κ .

† Equations (7) and (8) are identical to Artman and Tannenwald's⁵ expressions, if $4\pi^2 D^2 / (13.56 + \pi^2 D^2 / L^2)$ is substituted for λ_0^2 .

Equation (10) has a pole at $\chi_m \pm \kappa = -3$ which simply indicates the resonance condition for a sphere as derived by Kittel.¹⁰ This can be verified from (2):

$$\chi_m \pm \kappa = \frac{p}{\sigma \pm 1} \quad (11)$$

Note that p and σ are either both positive or both negative, hence, only one of the two quantities $(\chi_m + \kappa)$ or $(\chi_m - \kappa)$ goes through resonance at $|\sigma| = 1$. A similar situation exists for $\chi_{ms} \pm \kappa_s$ expressed in terms of (11)

$$\chi_{ms} \pm \kappa_s = \frac{3p}{p + 3(\sigma \pm 1)} \quad (12)$$

One of the two quantities $(\chi_{ms} \pm \kappa_s)$ goes through resonance at

$$|\sigma|_s = 1 - |p|/3 \quad (13)$$

Observing that the field in the sphere is given by (9) this may be written as

$$\frac{\omega_r}{|\gamma|} = H_z + M_z/3 = H_z^0 \quad (14)$$

(Kittel's resonance frequency of a ferrite sphere)

It is easily seen that this resonance of the spherical sample makes the evaluation of χ_m and κ from (10) rather unattractive because one would expect inaccurate results for χ_m and κ in the vicinity of the sphere resonance σ_s . Furthermore, for all numerical computations (10) must be separated into real and imaginary parts

$$\chi_{ms}' \pm \kappa_s' = 3 \frac{(\chi_m' \pm \kappa' + 3)(\chi_m' \pm \kappa') + (\chi_m'' + \kappa'')^2}{(\chi_m' \pm \kappa' + 3)^2 + (\chi_m'' \pm \kappa'')^2} \quad (15)$$

$$\chi_{ms}'' \pm \kappa_s'' = 9 \frac{\chi_m'' \pm \kappa''}{(\chi_m' \pm \kappa' + 3)^2 + (\chi_m'' \pm \kappa'')^2} \quad (16)$$

In general higher order terms of χ_m'' and κ'' may be neglected, but in the vicinity of sphere resonance these terms predominate as the term $\chi_m' \pm \kappa' + 3$ vanishes. It can be seen from the preceding discussion that the determination of χ_m' , χ_m'' , κ' , and κ'' from χ_{ms} and κ_s has its difficulties. Fortunately, there is an easier way to the interpretation of χ_{ms} and κ_s in terms of the intrinsic parameters χ_m and κ . We use (9) to define a new quantity σ' in terms of the applied magnetic field.

$$\sigma' = \sigma + p/3 = |\gamma| H_z^0 / \omega \quad (17)$$

Now (12) may be written in terms of the normalized applied static field as

$$\chi_{ms} \pm \kappa_s = \frac{p}{\sigma' \pm 1} \quad (18)$$

Comparison with (11) shows that the functional dependency of the effective parameters χ_{ms} and κ_s on the applied field H_z^0 is identical to Polder's relations for $\chi_m \pm \kappa$. This permits plotting $\chi_{ms} \pm \kappa_s$ versus H_z^0 and relabeling the coordinates $\chi_m \pm \kappa$ and H_z , provided that Polder's equations hold exactly. It would appear however that one of the reasons for measuring ferrite parameters is the fact that Polder's equations are known to be approximations which do not always hold and which are subject to many restrictions as pointed out earlier in this paper. Summing up, one may say that measurements of the parameters of a small ferrite sphere lead to excellent results in terms of effective quantities χ_{ms} and κ_s as a function of the applied static field, but may only be approximations when interpreted in terms of the intrinsic parameters χ_m and κ .

3.2 The Thin Disc Method

The use of a thin disc rather than a small sphere as a cavity perturbation eliminates most of the difficulties enumerated in the previous section because the intrinsic parameters $\chi_m \pm \kappa$ are measured directly. Placing a thin disc against the endwall of a cylindrical TE_{111} mode cavity (Fig. 3) and observing the splitting of the resonance frequency and change in $1/Q$ as before one obtains the following relationships (see Appendix for derivation)

$$\frac{\Delta\omega_{\pm}}{\omega_0} = \frac{1}{4} \frac{\lambda_0^2 t}{L^3} (\chi_m' R_1 \pm \kappa' R_2) \quad (19)$$

$$\Delta \left(\frac{1}{Q} \right)_{\pm} = \frac{1}{2} \frac{\lambda_0^2 t}{L^3} (\chi_m'' R_1 \pm \kappa'' R_2) \quad (20)$$

The quantity t denotes the thickness of the disc, and R_1 and R_2 are functions of the geometry which take into account that the RF magnetic field is not constant over the face of the disc. A plot of R_1 and R_2 versus the ratio of disc diameter to cavity diameter (Fig. 4) shows that the functions are closely equal for disc diameters less than $\frac{1}{2}D$. This implies circular polarization of the magnetic field in this region whereas the field becomes elliptically polarized as one approaches the outer diameter of the cavity. It might be argued that the disc should be small enough

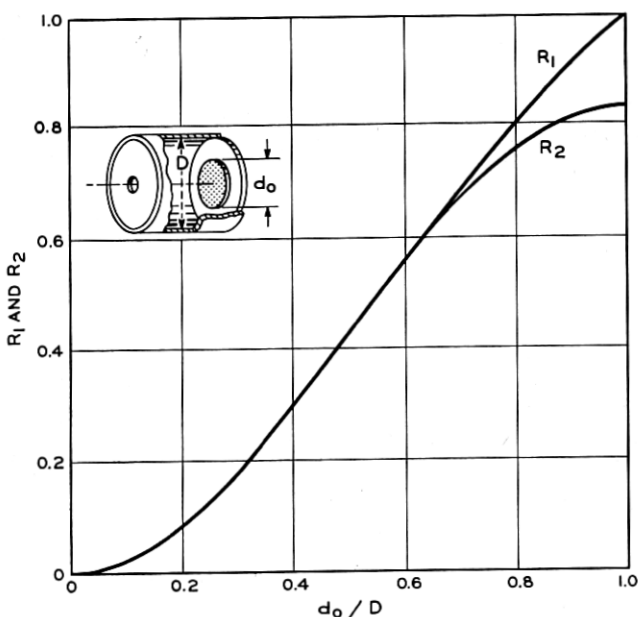


Fig. 4 — The functions R_1 and R_2 versus the ratio of disc diameter d_0 to cavity diameter D .

to be entirely within the circularly polarized region. However, this requirement appears to assume that there is some interaction, such as spinwave coupling, between adjacent regions in the disc. It is possible that such interaction exists in single crystals and leads to multiple resonance effects. However in polycrystalline material it is safe to assume that each crystallite reacts independently with the RF magnetic field, enabling us to sum these effects by simple integration.

This integration has been performed in the derivation of (19) and (20) under the assumption that the disc is thin enough to introduce only a first order perturbation into the cavity field. It will be shown presently that these assumptions are consistent with experimental results.

The measured effects $\Delta\omega_{\pm}$ and $\Delta(1/Q)_{\pm}$ depend on the volume of the perturbing body, hence one would expect that these effects are at least an order of magnitude larger for thin discs than for small spheres. This permits very accurate measurement of ferrite parameters in the region below saturation and below and above resonance. In particular, the loss parameters $\chi_m'' \pm \kappa''$ of modern low-loss ferrites can be determined accurately in these regions. However, in the resonance region, the measured effects become so large that measurement becomes difficult. Hence,

we do not recommend this method for measurement of resonance linewidth. The greatest advantage of the thin disc method lies in its ability to explore the region below resonance where many ferrite devices operate. It will be noted that this region is wider for the disc than for a small sphere or for a thin cylinder magnetized normal to its axis. Using Kittel's relations we find the field in the ferrite at which resonance occurs for a given saturation magnetization and operating frequency

$$\begin{array}{lll}
 H_{\text{res}} = \frac{\omega}{|\gamma|} & H_{\text{res}} = \frac{\omega}{|\gamma|} - \frac{M_s}{3} & H_{\text{res}} = \frac{\omega}{|\gamma|} - \frac{M_s}{2} \\
 \text{Thin Disc} & \text{Small Sphere} & \text{Thin Cylinder}
 \end{array} \quad (21)$$

It is seen that for some materials a small sphere or a thin cylinder may be at resonance even before it is saturated.

4. METHODS FOR MEASURING THE DIELECTRIC PROPERTIES

In principle the electric susceptibility χ_e may be measured with any of the three sample shapes discussed above provided the sample is placed into a region of maximum electric and vanishing magnetic field, e.g., the center of a TE_{111} mode cylindrical cavity. A simple computation shows that a small sphere located at the center of the cavity produces a frequency shift and change in $1/Q$ as follows:

$$\frac{\Delta\omega}{\omega_0} = 4.189 \frac{\chi_e'}{\chi_e' + 3} \cdot \frac{d_0^3}{D^2L} \quad (22)$$

$$\Delta(1/Q) = 25.136 \frac{\chi_e''}{(\chi_e' + 3)^2} \cdot \frac{d_0^3}{D^2L} \quad (23)$$

In actual measurements it is found that the dielectric constant is not entirely independent of the diameter of the sphere, and that the measurement of the loss factor χ_e'' is difficult because the change in $1/Q$ is very small. An additional inherent difficulty of this method is the fact that (22) is rather insensitive to large values of χ_e as are frequently encountered with ferrites. Again the thin disc method permits greater ease of measurement, larger effects, and a simpler relationship between the observed quantities and χ_e . We find (see Appendix A)

$$\frac{\Delta\omega}{\omega_0} = \chi_e' \frac{t}{L} R_1 \quad (24)$$

$$\Delta(1/Q) = 2\chi_e'' \frac{t}{L} R_1 \quad (25)$$

5. INSTRUMENTATION

Our measurement technique has been influenced by a number of practical considerations including the need for determining accurately and quickly a figure of merit for a large number of different ferrite materials. In particular, a variety of low loss materials has become available in experimental quantities requiring a precise technique for measuring small loss factors below resonance as a guide for further ferrite development. Therefore we were faced with the problem to develop an instrumentation capable of measuring these small loss factors but simple enough to be operated without detailed knowledge of microwave techniques. Fortunately the use of thin discs permits us to introduce a fairly large volume of ferrite into the cavity without violating the basic assumption of a small perturbation. As a consequence frequency shifts of the order of 10 mc are obtained at static magnetic fields just sufficient to saturate the material. Thus the quantities χ_m' and κ' may be measured without difficulty in the regions below and above resonance.

The thickness of the disc should be chosen to attain an aspect ratio (diameter/thickness) of 50 or larger. Discs of 0.005 to 0.007-inch thickness were employed in actual measurements at 9200 mc. For a typical measurement of a 0.005-inch disc at 9200 mc, a change of $1/Q$ of about 2 per cent corresponds to a loss term $\chi_m'' + \kappa'' = 2 \times 10^{-3}$. Measurement of Q with a reproducibility of 1 per cent has been accomplished initially by careful work, and it has been our objective to maintain this accuracy in routine measurements by semiskilled operators. This required the use of rather elaborate circuitry for the precise measurement of the changes in $1/Q$ of the cavity. Although most of these techniques have been used before in the field of microwave spectroscopy we hope that the description of this instrumentation will be of interest.

Fig. 5 shows a block diagram of the circuit. A klystron Type V58 (Varian Associates) is swept through a frequency band of about 80 mc at X-band. The resulting signal with a center frequency of 9,200 mc is used to excite a TE_{111} mode cylindrical cavity. Incident and reflected signals are separated by means of directional couplers and displayed on an oscilloscope. Both signals can be aligned with the aid of a shorting gate and a precision attenuator in front of the cavity. The reflected signal shows clearly the cavity resonance which splits into two if a ferrite disc is placed against the endwall of the cavity and magnetized along the cavity axis.

One of the major problems of the measurement is the accurate determination of these new cavity resonance frequencies and of the line width of the displayed resonance curves between half-power points. In the

solution of this problem, more than ordinary emphasis was placed on ease of operation and elimination of ambiguities in the frequency determination. The resulting instrumentation uses as a stable reference frequency a crystal-controlled oscillator and a frequency multiplier which yields three reference frequencies; 55.8, 223.3 and 4,020 mc. These are mixed in a crystal harmonic generator and mixer leading to a line spectrum of numerous reference frequencies with a constant spacing of 55.8 mc. The same crystal mixer produces a beat frequency signal between the incident signal from the klystron and each of these reference frequencies. A communication receiver with modified IF stage permits selection of a frequency marker out of these beat frequency signals. This marker appears as a blank spot on the traces of incident and reflected signal, and can be moved to any desired point by simply changing the frequency setting of the receiver. Since the receiver dial cannot be read with great accuracy on the high frequency ranges, a frequency counter connected with the local oscillator of the receiver permits a reading of the oscillator frequency to an accuracy of 1 keps. Noting that the local oscillator is 0.455 mc removed from the difference signal, one obtains the frequency of the difference signal with more than sufficient accuracy.

6. Results of Measurements

Transmission- and reflection-type cylindrical cavities have been employed for measurements with linearly and circularly polarized excitation in the 6,000- and 9,000-mc frequency bands. Circular polarization is preferable in the region below saturation where frequency shifts are small.

It is not necessary to choose ferrite discs of relatively small diameter for the purpose of staying within the region of circular polarization close to the cavity axis. The derivation of $\chi_m \pm \kappa$ is not restricted to circularly polarized fields, and the result takes into account that the field becomes more and more elliptically polarized as one approaches the edge of the cavity. This can be seen by rewriting (19) and (20) as follows:

$$\chi_m' \pm \kappa' = \frac{1}{\omega_0 F R_1 R_2} [\Delta\omega_{\pm} (R_1 + R_2) - \Delta\omega_{\mp} (R_1 - R_2)]$$

$$\chi_m'' \pm \kappa'' = \frac{1}{2FR_1R_2} [\Delta(1/Q)_{\pm}(R_1 + R_2) - \Delta(1/Q)_{\mp}(R_1 - R_2)] \quad (26)$$

where $F = t\lambda_0^2/(2L^3)$.

The factor $(R_1 - R_2)$, which is zero for circular polarization, corrects the values for $\chi_m \pm \kappa$ if the disc extends into the region of elliptical

polarization. For relatively small discs ($R_1 = R_2$), one obtains

$$\begin{aligned}\chi_m' \pm \kappa' &= \frac{2}{\omega_0 F R_1} \Delta\omega_{\pm} \\ \chi_m'' \pm \kappa'' &= \frac{1}{F R_1} \Delta(1/Q)_{\pm}\end{aligned}\tag{27}$$

A large number of measurements was made with a half-wave, reflection-type cavity and linearly polarized excitation. Some typical results will be discussed below to demonstrate the applicability of the disc technique. The frequency shift measurements and $\chi_m' \pm \kappa'$ for a ferrite material of 1,300 oersted saturation magnetization are shown on Fig. 6. The ferrite disc has a thickness of 0.0063 inch and completely covers the endwall of the cavity. If the field in the cavity were circularly polarized throughout, then the frequency shift would vary as $\chi_m' \pm \kappa'$. However, elliptical polarization causes a deviation of the measured curves for $\Delta\omega_{\pm}$ from $\chi_m' \pm \kappa'$. Agreement between theoretical and experimental values of $\chi_m' \pm \kappa'$ is good in the regions below and above resonance. Measurements in the resonance region are not possible with a disc of this size because frequency shift and change in Q are so large that the assumption of a small perturbation is violated. In order to establish further that measurements of $\chi_m' \pm \kappa'$ are independent of disc diameter three discs of the same material (saturation magnetization 1300 oersted) with diameters of 0.249, 0.400, and 1.050 inches were measured in the above-mentioned cavity. Plots of χ_m' and κ' (Fig. 7) indicate good agreement for κ' and some scattering of values for χ_m' . This can be explained by noting that the resonance frequency of the empty cavity enters into the computation of χ_m' , but cancels out for κ' (equation 19). Consequently, a very small change in the length of the cavity, as might be expected from opening and reassembling the device, will produce a noticeable error in the low-field region. A change in cavity length of 10^{-4} inch will produce a frequency shift of 1 mc at an operating frequency of 10,000 mc and introduce an error of the order of 0.02 into the measurement of χ_m' . This error may be minimized by using a relatively large disc.

Discs with a diameter of 0.4 inch yielded good measurements of the imaginary quantities $\chi_m'' \pm \kappa''$ in the low-field region. A typical result for a low-loss ferrite (Fig. 8) shows the measured quantities $\Delta(1/Q)_{\pm}$ and the corresponding $\chi_m'' \pm \kappa''$ as a function of the applied magnetic field. (The internal field in the ferrite is obtained by subtracting the magnetization from the applied field). It is noted that only $\Delta(1/Q)_{-}$ can be observed in the resonance region, whereas $\Delta(1/Q)_{+}$ becomes too

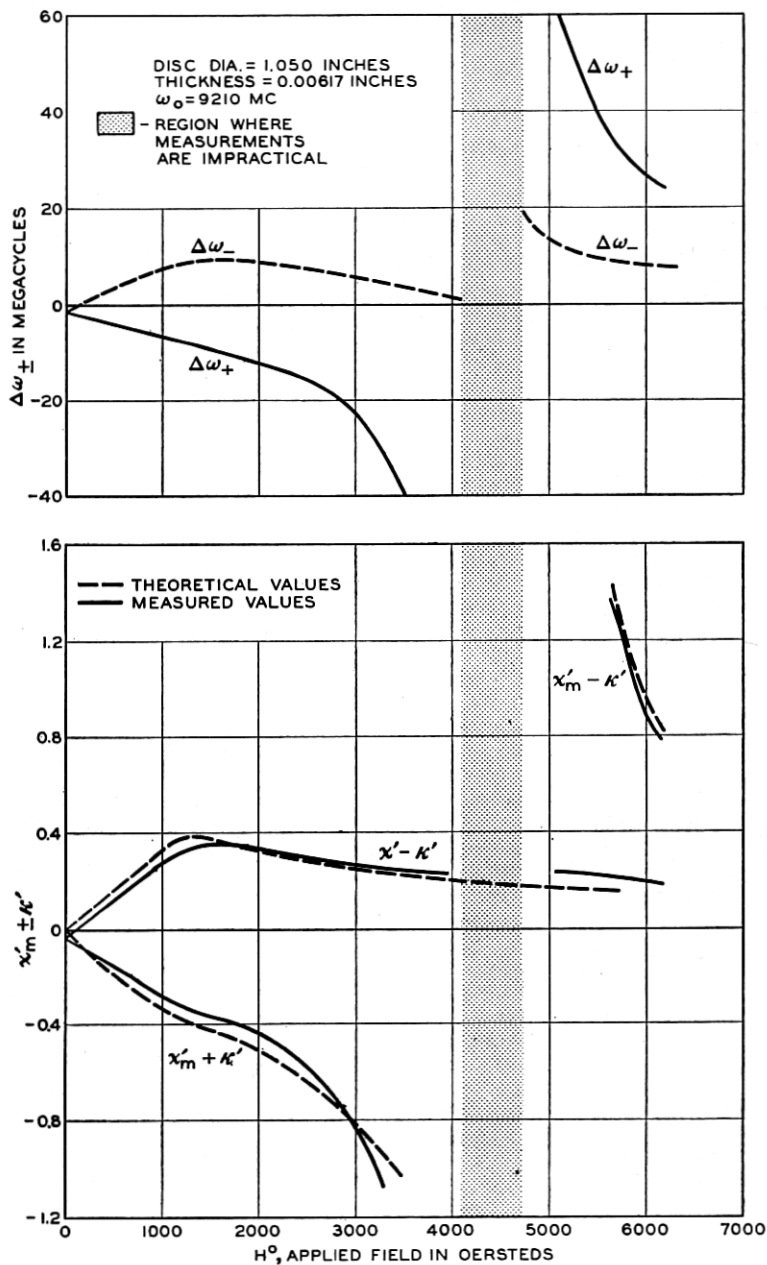


FIG. 6 — Evaluation of $\chi'_m \pm \kappa'$ from measurements of frequency shift $\Delta\omega_{\pm}$ and comparison with Polder's theory. Low-loss BTL ferrite, saturation magnetization 1300 oersted.

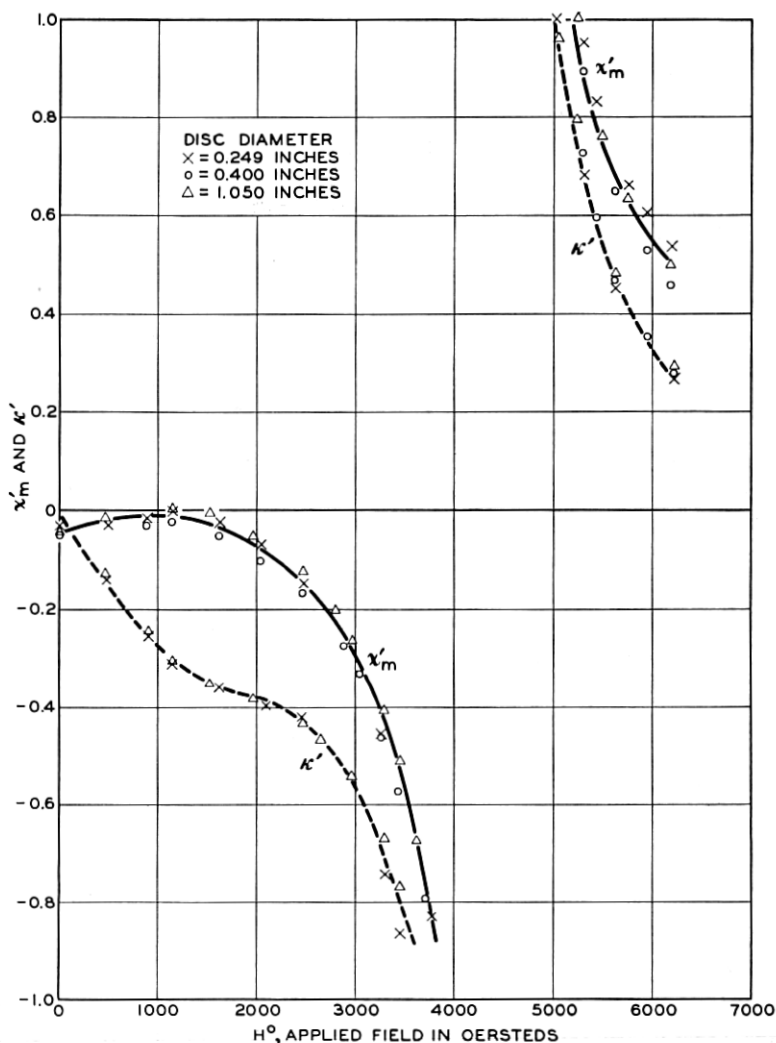


FIG. 7 — Measurement of χ'_m and κ' versus applied static field for three different discs, cut from the same ferrite block.

large to be measured. Knowledge of $\Delta(1/Q)_-$ is not sufficient to determine $\chi''_m - \kappa''$ in the resonance region because here the correction term $\Delta(1/Q)_+(R_1 - R_2)$ (cf. equation 26) becomes comparable to the term $\Delta(1/Q)_-(R_1 + R_2)$ and is needed to compensate for the anomalous peak of the $\Delta(1/Q)_-$ curve. The loss parameters $\chi''_m \pm \kappa''$ assume values of the order of 10^{-2} below and above resonance. The estimated error of the measurement is 3×10^{-3} .

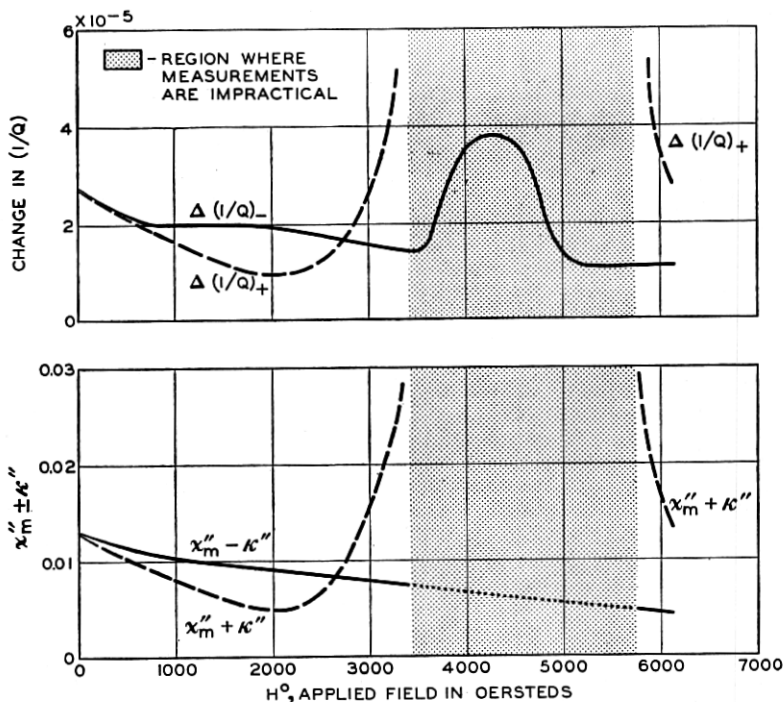


FIG. 8 — Evaluation of $\chi_m'' \pm \kappa''$ from measurements of $\Delta(1/Q)_{\pm}$ for low-loss BTL ferrite, saturation magnetization 1300 oersted.

Whereas it is possible to obtain good agreement between measured and theoretical curves of $\chi_m' \pm \kappa'$ from Polder's relations (3), such an agreement cannot be obtained for $\chi_m'' \pm \kappa''$ from a comparison with (4). This discrepancy is assumed to be caused by the fact that Polder's theory was developed for single ferrite crystals and did not take into account the random orientation of crystal axes in polycrystalline materials, such as the ferrites used in these measurements. It is reasonable to expect a broadening of the resonance line and a departure from the Lorentzian shape in polycrystalline ferrites; hence, the expression for the absorption line (4) no longer holds.

Measurement of the electric susceptibility of ferrites did not present any major difficulties, provided some care was used in the suspension of the discs at the cavity center.

Summing up these results it may be said that the disc method has yielded satisfactory measurements of the intrinsic parameters of polycrystalline ferrites below and above resonance as well as in the un-

saturated region. Measurements of single crystals and of resonance curves with this method have not yet been made.

It is anticipated that in both cases smaller and thinner discs would be needed than have been available so far. However, it can be hoped that these difficulties will be overcome in the near future and that the disc method will be useful also for the study of ferromagnetic resonance phenomena.

APPENDIX

PERTURBATION OF A DEGENERATE CYLINDRICAL CAVITY DUE TO A THIN DISC

The general perturbation equation for a lossless cavity can be derived from energy considerations or directly from Maxwell's equations. We obtain for the shift of resonance frequency due to a small perturbation:

$$2 \frac{\omega_0 - \omega_1}{\omega_0} = \frac{\frac{\mu_0}{2} \int_{v_1} \vec{m} \cdot \vec{h}^{0*} dv + \frac{1}{2} \int_{v_1} \vec{P} \cdot \vec{E}^{0*} dv}{\frac{\mu_0}{2} \int_{v_2} \vec{h}^0 \cdot \vec{h}^{0*} dv} = \frac{W_m^{(s)} + W_e^{(s)}}{W^{(c)}} \quad (\text{A1})$$

ω_0 resonance frequency of the empty cavity

ω_1 resonance frequency of the cavity after insertion of the perturbing sample

\vec{h}^0 magnetic field intensity vector in the empty cavity

\vec{E}^{0*} electric field intensity vector in the empty cavity

v_1 volume of sample

v_2 volume of cavity

* indicates the conjugate value

The denominator in (A1) indicates the total energy $W^{(c)}$ stored in the empty cavity at resonance, whereas the numerator is equal to the additional magnetic energy $W_m^{(s)}$ and electric energy $W_e^{(s)}$ stored in the perturbing sample.

Equation (A1) is valid if the frequency shift is small,

$$\frac{\Delta\omega}{\omega_0} = \left| \frac{\omega_1 - \omega_0}{\omega_0} \right| \ll 1 \quad (\text{A2})$$

and if the field in the cavity remains essentially unchanged after insertion of the sample. In order to apply (A1) to the determination of the tensor components χ_m and κ we should attempt to satisfy three conditions: the electric field should vanish at the sample, the magnetic field should be normal to the static magnetic field, and the relationship between RF

magnetization \vec{m} and RF magnetic field \vec{h}^0 in the cavity should be simple. All three conditions can be satisfied if a thin ferrite disc is placed against the endwall of the cavity (Fig. 3). Noting that the tangential component of the magnetic field intensity is continuous at the plane face of the disc we have:

$$\begin{aligned} m_r &= \chi_m h_r^0 - j\kappa h_\theta^0 \\ m_\theta &= j\kappa h_r^0 + \chi_m h_\theta^0 \end{aligned} \quad (\text{A3})$$

Inserting (A3) into (A1) we find the additional magnetic energy stored in the disc

$$W_m^{(s)} = \frac{\mu_0}{2} \int_{\tau_1} [\chi_m (h_r^0 h_r^{0*} + h_\theta^0 h_\theta^{0*}) + j\kappa (h_r^0 h_\theta^{0*} - h_\theta^0 h_r^{0*})] dv \quad (\text{A4})$$

In order to evaluate (A4) we use the fact that the TE_{III}-mode can be expressed as the sum of two circularly polarized modes rotating in opposite directions

$$\begin{aligned} \vec{h}^0 &= \vec{h}_1^0 + \vec{h}_2^0 \\ \vec{E}^0 &= \vec{E}_1^0 + \vec{E}_2^0 \end{aligned} \quad (\text{A5})$$

Thus, we have

$$\begin{aligned} h_{r1,2}^0 &= B \frac{\beta}{k_c} J_1'(k_c r) e^{\pm j\theta} \cos \beta z \\ h_{\theta 1,2}^0 &= \pm jB \frac{\beta}{k_c^2 r} J_1(k_c r) e^{\pm j\theta} \cos \beta z \end{aligned} \quad (\text{A6})$$

$$\begin{aligned} h_{z1,2}^0 &= BJ_1(k_c r) e^{\pm j\theta} \sin \beta z \\ E_{r1,2} &= \pm B \frac{\omega \mu_0}{k_c^2 r} J_1(k_c r) e^{\pm j\theta} \sin \beta z \end{aligned} \quad (\text{A7})$$

$$E_{\theta 1,2} = jB \frac{\omega \mu_0}{k_c} J_1'(k_c r) e^{\pm j\theta} \sin \beta z$$

B	amplitude factor
J_1	Bessel function of the first kind
$\beta = (\beta_0^2 - k_c^2)^{\frac{1}{2}}$	propagation constant in the z -direction
$k_c = p_1'/a$	propagation constant in the r -direction
$\beta_0 = 2\pi/\lambda_0$	propagation constant in free space
L	length of cavity
λ_0	wavelength in free space
a	radius of cavity
$\lambda_g = 2L$	wavelength in the cavity
$p_1' = 1.841$	first zero of the derivative of J_1

Integration of the electric or magnetic field over the volume of the cavity yields the stored energy in the empty cavity at resonance for one of the two circularly polarized modes

$$W^{(c)} = 0.2387 \frac{\pi\mu_0}{4} \cdot \frac{\beta_0^2}{k_c^2} B^2 a^2 L \quad (\text{A8})$$

The magnetic energy $W_m^{(s)}$ in the disc is found by integrating (A4) over the volume of the disc and assuming that the field is constant over the thickness t of the disc. We obtain:

$$W_m^{(s)} = 0.2387 \frac{\pi\mu_0 \beta^2}{2 k_c^2} B^2 a^2 t (\chi_m R_1 \pm \kappa R_2) \quad (\text{A9})$$

The two functions R_1 and R_2 depend on the ratio of disc radius to cavity radius

$$R_1 = 4.1893 \frac{r_0^2}{a^2} \left[(J_0(k_c r_0))^2 + \left(1 - \frac{2}{(k_c r_0)^2} \right) (J_1(k_c r_0))^2 \right] \quad (\text{A10})$$

$$R_2 = 2.4720 (J_1(k_c r_0))^2 \quad (\text{A11})$$

It is interesting to note that these two functions are approximately equal (Fig. 4) if the disc radius is less than half the cavity radius. In this region the field in the cavity is essentially circularly polarized, whereas elliptical polarization exists near the wall of the cavity. Inserting (A8) and (A9) into (A1) we find the desired relationship between the two frequency shifts associated with positive and negative circular polarization and the tensor components χ_m and κ .

$$2 \frac{\Delta\omega_{\pm}}{\omega_0} = \frac{1}{2} \frac{\lambda_0^2 t}{L^3} (\chi_m R_1 \pm \kappa R_2) \quad (\text{A12})$$

Equations (A1) and (A12) hold for complex χ_m and κ if a complex frequency shift is introduced as follows:

$$d\bar{\omega} = \omega - \omega_0 + j(\alpha - \alpha_0) \quad (\text{A13})$$

The attenuation constant α may be defined in terms of the internal Q of the cavity, $\alpha = \frac{1}{2}\omega/Q$ and the internal Q is defined as

$$Q = \frac{\omega(\text{energy stored in circuit})}{\text{average power loss}}$$

Thus, the imaginary part of the frequency shift may be expressed as the difference between $(1/Q)$ of the perturbed cavity at the new resonance frequency ω and $(1/Q_0)$ referring to the empty cavity at ω_0 .

$$\Delta(1/Q) = \frac{1}{Q} - \frac{1}{Q_0} = 2 \frac{(\alpha - \alpha_0)}{\omega_0} \quad (\text{A14})$$

We note that the imaginary part of the right hand side of (A1) does indeed represent the power dissipation in the perturbing sample over the stored energy times ω . Hence, taking the imaginary part of (A12)

we have a relationship between the change in $(1/Q)$ and the loss terms χ_m'' and κ''

$$\Delta(1/Q)_{\pm} = \frac{1}{2} \frac{\lambda_0^2 t}{L^3} (\chi_m'' R_1 \pm \kappa'' R_2) \quad (\text{A15})$$

Clearly, (A15) holds only if the initial Q of the empty cavity is very high and the change in Q is quite small.

The electric susceptibility of the ferrite disc can be obtained in a similar way, provided we place the disc at the cavity center where the electric field has a maximum. Then, the additional electric energy stored in the disc is found to be

$$W_e^{(s)} = 0.2387 \frac{\pi}{2} \mu_0 \chi_e \frac{\beta_0^2}{k_c^2} B^2 a^2 t R_1 \quad (\text{A16})$$

It should be noted that there is an important difference between location of a thin disc at the endwalls and at the center of a cylindrical cavity. Whereas the electric field at the endwall may be neglected entirely, the magnetic field at the cavity center has a component parallel to the cavity axis. The effect of this component on the stored energy in the disc may be minimized by magnetizing the disc beyond saturation in the z -direction.

With the assumption that the effects of the magnetic RF field may be neglected we obtain relationships for the electric susceptibility and electric loss factor:

$$2(\Delta\omega/\omega_0) - j\Delta(1/Q) = (\chi_e' - j\chi_e'') \frac{2t}{L} R_1 \quad (\text{A17})$$

Since χ_e is a scalar quantity there is no splitting of the cavity resonance.

ACKNOWLEDGMENT

We would like to thank L. G. Van Uitert who supplied the ferrite materials, Barbara De Hoff who did all of the numerical computation and Edward Kankowski who made most of the measurements shown herein.

REFERENCES

1. D. Polder, *Phil. Mag.*, **40**, p. 99, 1949.
2. C. L. Hogan, *Rev. Mod. Phys.*, **25**, p. 253, 1953.
3. H. Suhl and L. R. Walker, *B.S.T.J.*, **33**, p. 579, 1954.
4. W. A. Yager, J. K. Galt, F. R. Merritt, and E. A. Wood, *Phys. Rev.*, **80**, p. 744, 1950.
5. J. O. Artman and P. E. Tannenwald, *J. Appl. Phys.* **26**, p. 1124, 1955.
6. A. D. Berk and B. A. Lengyel, *Proc. I.R.E.*, **43**, p. 1587, 1955.
7. A. A. Th. M. Van Trier, *Appl. Sci. Res.*, **3**, p. 305, 1953.
8. J. Stratton, *Electromagnetic Theory*, Chapter 1, McGraw-Hill Book Co., New York, 1941.
9. J. H. Rowen and W. von Aulock, *Phys. Rev.*, **96**, p. 1151, 1954.
10. C. Kittel, *Phys. Rev.*, **73**, p. 155, 1948.